



# HHS Public Access

Author manuscript

*Environ Sci Technol.* Author manuscript; available in PMC 2019 March 06.

Published in final edited form as:

*Environ Sci Technol.* 2018 March 06; 52(5): 2844–2853. doi:10.1021/acs.est.7b04889.

## Mobile and Fixed-Site Measurements To Identify Spatial Distributions of Traffic-Related Pollution Sources in Los Angeles

Mei W. Tessum<sup>\*,†,‡,iD</sup>, Timothy Larson<sup>†,‡</sup>, Timothy R. Gould<sup>‡</sup>, Christopher D. Simpson<sup>†</sup>, Michael G. Yost<sup>†</sup>, and Sverre Vedal<sup>†</sup>

<sup>†</sup>Department of Environmental and Occupational Health Sciences, University of Washington, Box 357234, Seattle, Washington 98198, United States


<sup>‡</sup>Department of Civil & Environmental Engineering, University of Washington, Box 352700, Seattle, Washington 98198, United States

### Abstract

Mobile monitoring and fixed-site monitoring using passive sampling devices (PSD) are popular air pollutant measurement techniques with complementary strengths and weaknesses. This study investigates the utility of combining data from concurrent 2-week mobile monitoring and fixed-site PSD campaigns in Los Angeles in the summer and early spring to identify sources of traffic-related air pollutants (TRAP) and their spatial distributions. There were strong to moderate correlations between mobile and fixed-site PSD measurements of both NO<sub>2</sub> and NO<sub>x</sub> in the summer and spring (Pearson's *r* between 0.43 and 0.79), suggesting that the two data sets can be reliably combined for source apportionment. PCA identified the major TRAP sources as light-duty vehicle emissions, diesel exhaust, crankcase vent emissions, and an independent source of combustion-derived ultrafine particle emissions. The component scores of those four sources at each site were significantly correlated across the two seasons (Pearson's *r* between 0.58 and 0.79). Spatial maps of absolute principal component scores showed all sources to be most prominent near major roadways and the central business district and the ultrafine particle source being, in addition, more prominent near the airport. Mobile monitoring combined with fixed-site PSD sampling can provide high spatial resolution estimates of TRAP and can reveal underlying sources of exposure variability.

### Graphical abstract

<sup>\*</sup>Corresponding Author. Phone: 612-986-3936; mtessum@uw.edu.

ORCID 

Mei W. Tessum: 0000-0003-0298-8529

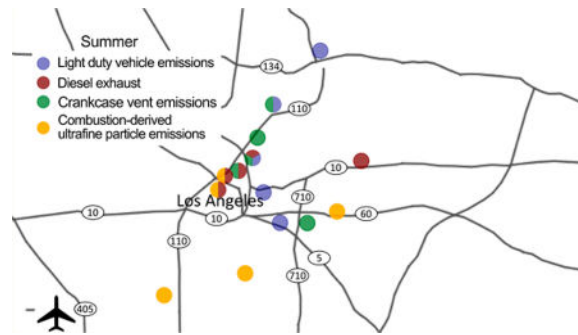
#### ASSOCIATED CONTENT

Supporting Information

The Supporting Information is available free of charge on the [ACS Publications website](https://pubs.acs.org) at DOI: 10.1021/acs.est.7b04889.

List of pollutants and their concentrations measured in the study (Tables S1, S4, S5), discussion of seasonal and regional differences of correlations between the mobile and fixed-site PSD data (Tables S2, S3, S6–S9, references), mobile platform background pollutant concentrations in Los Angeles and Baltimore (Table S10), and maps of absolute PCA component score percentiles associated with certain types of roadways (Figures S1 and S2) ([PDF](#))

The authors declare no competing financial interest.



## INTRODUCTION

Concentrations of traffic-related air pollutants (TRAP) typically have large spatial gradients near roadways.<sup>1</sup> Therefore, monitoring air quality at high spatial resolution is desirable for TRAP, especially in estimating long-term population exposures. Traditional stationary monitoring is usually not able to provide sufficient spatial resolution to precisely estimate the contribution of traffic to ambient pollutants, such as fine particulate matter, black carbon, and  $\text{NO}_x$ , and may result in significant exposure measurement error.<sup>1</sup>

Mobile monitoring has been increasingly employed to measure small spatial scale variation in air pollutant concentrations.<sup>2–10</sup> A variety of sampling equipment (from simple portable devices to a highly sophisticated array of instruments), sampling platforms (e.g., pedestrians, bicycles, buses, or cars), amounts of traffic, and locations (e.g., freeways, arterial roads, or residential streets) has been used in these studies, demonstrating the utility of mobile monitoring in a number of settings and for addressing different scientific hypotheses.

Along with these advantages come some disadvantages to mobile monitoring. Because monitoring is not done at any point for an extended period of time, it is challenging to use it to identify temporal trends or temporal variations in concentrations. Further, because measurements at different points in space occur at different times, one has little assurance that apparent differences in space are not simply due to differences in time. That is, spatial measurements are confounded by time, and temporal measurements are confounded by space. Recent studies have recognized this issue and have suggested methods to adjust temporal variation and to increase the ability of mobile measurements to quantify spatial variation in longer-term average concentrations.<sup>11–16</sup>

Monitoring TRAP at both high spatial and temporal resolution is desirable. Combined mobile and fixed-site measurements with rich spatial and temporal information can reveal underlying TRAP sources of exposure variability. Sullivan and Pryor, for example, successfully combined mobile and fixed-site measurements to examine the spatiotemporal variability of short-term  $\text{PM}_{2.5}$  measurements, albeit in a small urban area.<sup>17</sup>

Calculating the correlation between temporally adjusted mobile measurements and fixed-site measurements can provide information about the extent to which the two sources of measurements agree. Van den Bossche et al. found moderate to strong correlations between mobile and stationary black carbon (BC) measurements in two small urban regions

(monitoring areas with perimeters of 2 and 5 km, respectively).<sup>5</sup> A study of a relatively large monitoring area conducted in Baltimore, MD, by Riley et al. found significant correlations between mobile measurements of NO<sub>x</sub>, BC, and four size ranges of particulate matter and passive sampler measurements of NO<sub>x</sub>, NO<sub>2</sub>, and various volatile organic compounds (VOCs).<sup>7</sup> Riley et al. also reported that adding mobile measurements to fixed-site PSD measurements allowed the extraction of additional multivariate TRAP source apportionment features.<sup>7</sup> However, previous mobile measurement studies have not identified spatial distributions of the TRAP sources, which could be useful in understanding and controlling TRAP.

In this study, mobile monitoring over a large area (approximately 40 × 58 km) and a passive sampling campaign covering the greater Los Angeles area were conducted in both summer and spring seasons. A principal components analysis (PCA) was performed on combined data from both platforms to identify the major traffic-related air pollution sources in Los Angeles. We created spatial maps of absolute principal component scores to visualize the spatial distributions of those sources and to examine the correlations of spatial patterns of those sources across seasons.

## METHODS

### Data Collection

Both mobile platform monitoring and fixed-site PSD campaigns were conducted during the spring (March 9–26, 2013) and summer (June 14–July 1, 2013) in Los Angeles. Forty-three fixed-site PSD sampling locations were selected throughout urban Los Angeles for a combination of residential streets and mixed traffic composition roadways. Mobile platform campaigns sampled in the immediate area surrounding these 43 locations following a cloverleaf pattern to create 43 corresponding “fuzzy points”, as shown in Figure 1. In this study, a fuzzy point refers to an area around an intersection of interest that contains all of the mobile measurements within a 300 m radius.

**Fixed-Site Campaigns Using Passive Sampling Devices (PSD)**—Fixed-site PSD campaigns were conducted March 9–24 and June 15–30, 2013. Over 2 weeks, integrated levels of NO<sub>2</sub>, NO<sub>x</sub>, and selected organic compounds (pentanes, benzene, toluene, *m*- and *o*-xylene, nonane, decane, and undecane) were measured at the 43 selected locations which were within a distance of approximately 2–8 m from the closest roadway intersection (shown as red circles in Figure 1). These locations will be referred to as the “intersections”. Ogawa samplers (Ogawa & Co., USA, Inc., Pompano Beach, FL) were used to measure NO<sub>2</sub> and NO<sub>x</sub> and were previously validated and described by Riley et al.<sup>7</sup> The Ogawa sampler contained two filters in separate chambers for measuring NO<sub>2</sub> (triethanol-amine coating) and NO<sub>x</sub> (2-phenyl-4,4,5,5-tetramethylimidazoline-3-oxide-1-oxyl coating), respectively. Eight organic compounds [those listed in Table S1 of the Supporting Information (SI)] were sampled using 3M organic vapor monitors with two charcoal adsorbent pads (3M Co., Saint Paul, MN). The monitors were uncapped upon arrival at the site and sealed with a design-fitting cap when the sampling finished.

During the measurement period, PSDs were attached to custom-built aluminum/stainless steel sampler shelters and were mounted on utility poles approximately 3 m above the ground. In each season, 9–10 duplicates as well as 9–10 field and laboratory blanks were deployed. After data collection, all samplers were returned to the Environmental Health Laboratory at the University of Washington for analysis. Detailed descriptions of the laboratory analyses are provided in the supplement to Riley et al.<sup>7</sup>

**Mobile Platform Campaigns**—Mobile campaigns were conducted March 10–26 and June 14–July 1, 2013, between the hours of 14:00 and 19:00. Each intersection was repeatedly visited by a gasoline-powered minivan (a 2012 model for the spring campaign and a 2013 model for the summer campaign) that was driven through each intersection at an average speed of 20 km/h from different directions. The route traveled is displayed in Figure 1. Mobile measurements taken within a 300 m radius of each PSD sample site were considered the measurements for that intersection or fuzzy point, as shown as blue circles in Figure 1. Each intersection was visited 4–5 times for an average of 10 min total sampling time. Measurements were recorded as 10-s averages. We collected an average of 275 measurements at each intersection across the two campaigns. This mobile measuring method has previously been described by Larson et al. and Riley et al.<sup>7,18,19</sup>

Particulate matter and gases (Table S1, SI) were separately sampled through two vehicle-roof-mounted inlets constructed of stainless steel/copper (for particle sampling) and Teflon (for sampling of gases). The particle inlet is designed to provide isokinetic sampling at a speed of 35 km/h. Data synchronization and logging were performed in the LabVIEW environment using LabVIEW 2010 with DAQmx 9.4 and NI serial 3.8 instrument drivers.<sup>19</sup>

The potential for emissions from the monitoring vehicle to contaminate mobile measurements (self-pollution) was tested using the approach described by Larson et al.<sup>20</sup> In brief, mobile fuzzy point measurements were classified into two categories based on vehicle speed: <2.3 km/h (idle or near idle) and ≥2.3 km/h (moving). PCA results for light-duty vehicle contributions were compared between idle or near-idle and moving conditions. No significant difference was found between the two categories, with a mean score difference (idle–moving) of 0.021 ( $p = 0.44$ ), suggesting a lack of self-pollution.

## Data Adjustment

Temporal trend adjustments were performed to address differences in concentration of pollutants measured at each intersection owing to between-day and within-day changes in pollutant emissions and dispersion. The mobile platform measurements of BC, CO, CO<sub>2</sub>, NO<sub>2</sub>, NO<sub>x</sub>, ultrafine particle number (UFPN, 25–400 nm; PN<sub>1</sub>, 50–1000 nm), and PN<sub>Intermodal</sub> (1–3 μm) were adjusted for between-day temporal trends by subtracting the daily fifth percentile as

$$\vec{C}_{i,\text{adjusted}} = \vec{C}_i - 5\text{th percentile}(\vec{C}_i) \quad (1)$$

where  $C \rightarrow_{i, \text{adjusted}}$  is the vector of all the adjusted concentrations on day  $i$ , and  $C \rightarrow_j$  is the vector of all observed concentrations on day  $j$ . This adjustment assumes that the lowest measurements across the sampling routes during the afternoon hours represents the well-mixed background concentration of Los Angeles. This type of adjustment is assumed to be less likely to alter the spatial relationships among the intersections than a rolling minimum adjustment would be.<sup>21</sup>

In addition, the mobile platform measurement of  $\text{PN}_{\text{fine}}$  (0.25–1  $\mu\text{m}$ ) was adjusted to account for within-day variability caused by regional transport. A 30 min rolling fifth percentile was subtracted from the  $\text{PN}_{\text{fine}}$  measurements as

$$\text{PN}_{\text{fine}, t, \text{adjusted}} = \text{PN}_{\text{fine}, t} - 5\text{th percentile}(\text{PN}_{\text{fine}, t-15} \dots \text{PN}_{\text{fine}, t+15}) \quad (2)$$

where  $\text{PN}_{\text{fine}, t, \text{adjusted}}$  is the adjusted count of particles with a diameter of 0.25–1  $\mu\text{m}$  at time  $t$ ,  $\text{PN}_{\text{fine}, t}$  is the observed  $\text{PN}_{\text{fine}}$  at time  $t$ , and  $\text{PN}_{\text{fine}, t-15} \dots \text{PN}_{\text{fine}, t+15}$  are the  $\text{PN}_{\text{fine}}$  measurements within a 30-min time period with a midpoint at time  $t$ . Details about the adjustment approaches used in this study, and their justification, are described in the supplement to Riley et al.<sup>7</sup> For the mobile monitoring data, the adjusted measurements can be zero or even negative, the latter representing the lowest fifth percentile concentrations among all measurements. Both the average and the median of mobile platform measurements for each pollutant before and after data adjustment are shown in the SI. The median of the mobile concentrations after data adjustment was used because it is insensitive to high concentration plumes in the distribution of concentrations measured at an intersection.

## Data Analysis and Data Processing

The mobile median concentration for each pollutant sampled during the 2-week period at each intersection across all days within a season was calculated to allow comparison with the corresponding PSD 2-week average concentration for each pollutant at each intersection within the same season. Pearson's correlation coefficients were estimated between medians of mobile campaign pollutants and averages of fixed-site PSD campaign pollutants.

PCA was used to identify relative source contributions above background. The traditional source apportionment approach typically does not involve a background adjustment of the data. In this study, however, only traffic sources rather than all sources are of interest. Therefore, sources of background concentrations are neglected. For this analysis, we combined both mobile and fixed-site data from both seasons because certain VOC measurements were missing from the winter campaign. Combining measurement sources and the summer and winter campaign data increases our ability to perform source-apportionment based on the relative source contributions above the background. Data were standardized by mean-centering and scaling by the variance before varimax-rotated principal components were calculated—including a normalized value for a zero concentration—using the following equations

$$Z_{i,p} = \frac{C_{i,p} - \overline{C_p}}{SD(C_p)} \quad (3)$$

and

$$Z_{0,p} = \frac{0 - \overline{C_p}}{SD(C_p)} \quad (4)$$

where  $Z_{i,p}$  is the normalized concentration of pollutant  $p$  (of  $np$  total pollutants) at location  $i$  (of  $n$  total measurement locations),  $C_{i,p}$  is measured concentration of pollutant  $p$  at location  $i$ ,  $\overline{C_p}$  is mean of the concentration of pollutant  $p$  across all locations,  $SD(C_p)$  is the standard deviation of the concentration of pollutant  $p$  across all locations,  $Z_{0,p}$  is the normalized concentration of pollutant  $p$  for a concentration of 0. Performing these calculations for  $n$  locations and  $np$  pollutants results in a  $\mathbf{Z}$  matrix of dimension  $(n, np)$  and a  $\mathbf{Z}_0$  matrix of dimension  $(1, np)$ .

The number of principal components to report was determined first by the Kaiser's stopping rule by which only the number of components with eigenvalues over 1 should be considered in the analysis. Pollutants with loadings of 0.55 or higher (i.e., those pollutants that contributed most to a profile) were considered in the analysis.<sup>22</sup>

Once the number of components had been decided, the PCA loadings of each component for each pollutant were multiplied with  $\mathbf{Z}$  and  $\mathbf{Z}_0$  using the following equations

$$\mathbf{S} = \mathbf{Z}\mathbf{L} \quad (5)$$

and

$$\mathbf{S}_0 = \mathbf{Z}_0\mathbf{L} \quad (6)$$

where  $\mathbf{L}$  is a  $(np, nc)$  matrix of PCA loadings,  $\mathbf{S}$  is a  $(n, nc)$  matrix of PCA scores at each location for each component (where  $nc$  is the number of PCA components), and  $\mathbf{S}_0$   $(1, nc)$  is a matrix of PCA scores for zero concentration values for each component. Then, the  $\mathbf{S}_0$  vector was subtracted from each row of the  $\mathbf{S}$  matrix to obtain absolute PCA scores. Finally, percentiles of the absolute PCA scores for each fuzzy point for each PCA component were mapped to visualize the distribution of the sources. The PCA loadings were applied to the normalized concentrations of pollutants in the summer and spring separately. The absolute principal component scores (APCS) map provides information about where the high loadings of pollutants of each component are located and therefore suggests spatial distributions of the pollution sources. Data analysis was performed using R.<sup>23</sup>

## RESULTS

### Summary of Fixed-Site and Mobile Platform Measurements

The distributions of fixed-site and mobile platform measurement results are shown in Figure 2, parts A and B, respectively. The NO<sub>2</sub>, NO<sub>x</sub>, and VOC concentrations in the spring fixed-site campaign were significantly higher than those in the summer fixed-site campaign (all  $p < 0.0001$ ). The summer concentrations of NO<sub>2</sub> and NO<sub>x</sub> measured by the fixed-site platform were  $15 \pm 3.4$  ppb (mean  $\pm$  SD) and  $25 \pm 4.6$  ppb, respectively, and were  $26 \pm 2.7$  and  $49 \pm 6.9$  ppb, respectively, in the spring. This seasonal difference in NO<sub>2</sub> concentrations was consistent with the Air Quality System (AQS) regulatory monitoring results for the same period of time at a relatively highly trafficked site in central Los Angeles (GPS 34.06659, -118.227) (the red lines shown in Figure 2).<sup>24</sup> Low molecular weight hydrocarbons (i.e., pentanes, benzene, and toluene) had higher concentrations than the long chain alkanes (i.e., nonane, decane, and undecane). The concentrations of all pollutants measured in the mobile campaign, except UFPN and PN<sub>1</sub>, were higher in the spring than the summer (all  $p < 0.0001$  using the paired  $t$  test). There was no significant seasonal difference in mobile UFPN and PN<sub>1</sub> measurements ( $p = 0.66$  and  $0.23$  using the paired  $t$  test, respectively).

### Correlations between Fixed-Site PSD and Mobile Platform Measurements

There were significant correlations between fixed-site NO<sub>2</sub> and NO<sub>x</sub> and mobile NO<sub>2</sub> and NO<sub>x</sub> in both summer and spring, respectively, as highlighted in the shaded areas in Tables S2 and S3 (SI). In the summer campaign, the mobile PN<sub>intermodal</sub> was correlated with fixed-site NO<sub>2</sub>, NO<sub>x</sub> and the long chain alkane VOCs. Black carbon and CO<sub>2</sub> were correlated with fixed-site NO<sub>2</sub> and NO<sub>x</sub>. In the spring campaign, mobile PN<sub>1</sub> and PN<sub>fine</sub>, black carbon, and CO<sub>2</sub> were correlated with fixed-site NO<sub>2</sub>. Mobile CO was correlated with fixed-site NO<sub>x</sub>, toluene, and *o*-xylene.

### Principal Components Analysis

Using combined summer and spring data, four PCA components were identified (Figure 3), explaining 83% of the total variance. As shown in Table 1, the first component or light-duty vehicle feature had high loadings ( $>0.55$ ) of low molecular weight hydrocarbons (i.e., pentanes, benzene, and toluene), xylenes, and passive NO<sub>x</sub>. The second component or diesel exhaust feature had high loadings of both mobile and passive NO<sub>2</sub> and NO<sub>x</sub>, CO<sub>2</sub>, BC, and PN<sub>fine</sub>. The third component or crankcase vent emission feature had high loadings of long-chain alkanes (i.e., nonane, decane, and undecane) and PN<sub>intermodal</sub>. The fourth component or ultrafine combustion particle feature had high loadings of BC, particle count of two ultrafine particle metrics (UFPN and PN<sub>1</sub>), and the difference between UFPN and PN<sub>1</sub>.

Figure 4 shows percentiles of PCA component scores for the summer and spring, respectively, at all intersections for all four PCA components. Larger and darker circles in the maps correspond to larger contributions to pollutant concentrations. In general, the first three principal components tended to have higher scores in the downtown area and along major highways, as expected. In the summer, the light-duty vehicle feature tended to have higher scores in the east of downtown, along Interstate 10 and along California State Route 60 in the eastern part of the city, and along Interstates 110 and 210 in the northeast part of

the city, while in the spring, these tended to be scattered around the southern part of the city, along Interstate 110, and between State Route 60 and Interstate 710. The diesel exhaust feature tended to have higher scores in downtown Los Angeles and along Interstate 10 and State Route 60 in the eastern part of the city in both spring and summer. The crankcase vent emissions feature tended to have higher scores in the north of downtown Los Angeles, along Interstates 10 and 110, and along Interstate 710 in the eastern part of the city in the summer, while in the spring, these tended to be along U.S. Route 101 in the western part of the city, and along Interstate 710 in the eastern part of the city. The combustion-derived ultrafine-particle-related air pollution feature tended to have high scores in the southern part of the city and in downtown Los Angeles, as well as in the southwest close to Los Angeles International Airport and along State Route 60 in the eastern part of the city in the summer, while in the spring scores for this component tended to be elevated in the southern part of the city and along Interstate 10, Interstate 710, and State Route 60 in the eastern part of the city. The component scores at each site were relatively highly correlated across the two seasons (Pearson's  $r = 0.58, 0.76, 0.79,$  and  $0.69$  for the four principal components, respectively).

## DISCUSSION

Comparing short-term mobile monitoring results against longer-term 2-week averages from stationary monitoring can provide information regarding the suitability of supplementing fixed-site measurements with short-term mobile monitoring campaigns in representing longer-term spatial patterns of TRAP and other sources.  $\text{NO}_x$  and  $\text{NO}_2$ —the only two pollutants measured in both the mobile and fixed-site campaigns—were significantly correlated in both seasons, providing evidence that repeated short-time mobile monitoring results can be used to reflect longer-term (at least 2 weeks) stationary monitoring results. This agreement provides confidence that combining mobile and fixed-site measurement data can provide useful information for multivariate analysis of source-related features. The use of very precise measurements of  $\text{NO}_2$  using the CAPS  $\text{NO}_2$  monitor compared to the less precise  $\text{NO}_x$  monitor may have contributed to the better correlations for  $\text{NO}_2$  than for  $\text{NO}_x$ . Riley et al. also reported correlations between mobile and fixed-site data using the same monitoring platform in Baltimore.<sup>7</sup> Seasonal (summer vs spring or winter) and regional (Los Angeles vs Baltimore) differences in the correlations are discussed in the SI.

The PCA indicated four prominent components. The first PCA component—with rich low molecular weight hydrocarbons (i.e., pentanes, benzene, and toluene), xylenes, and  $\text{NO}_x$  features—is identified as a light-duty vehicle source. This is consistent with the finding that gasoline-fueled vehicles appear to be the dominant source of C2–C9 hydrocarbons and CO in California.<sup>25</sup> Although CO is often considered an indicator of gasoline emissions,<sup>26</sup> the lack of correlation between CO and other pollutants (Tables S6 and S7, SI)—which may be caused by a relatively high background level—may have limited the contribution of CO to the components identified. Therefore, the relative contribution of CO for the PCA loadings is lower than reported by Riley et al.<sup>7</sup> The second PCA component—with rich  $\text{NO}_2$ ,  $\text{NO}_x$ ,  $\text{CO}_2$ , BC, and  $\text{PN}_{\text{fine}}$  features—is identified as a diesel exhaust source, which is consistent with findings of previous studies.<sup>26–28,20</sup> The locations with higher percentiles of PCA component scores in the second PCA component tended to be within 500 m of truck routes



(Figure S1, SI), supporting the conclusion that this component is indicative of diesel exhaust. The third component—with rich long-chain alkanes (i.e., nonane, decane, and undecane) and  $PN_{intermodal}$ —is suggestive of a crankcase vent emissions source: Zielinska et al. found greater organic carbon emissions from the crankcase than from the tailpipe.<sup>29</sup> Those organic carbons, especially long-chain alkanes (C7–C8), were mainly found in lubricating oil. Shirmohammadi et al. emphasized the importance of nontailpipe emissions in Los Angeles, especially after the reductions of diesel tailpipe emissions caused by control policies in recent years in California.<sup>30</sup> The fourth component is rich in BC, the particle count of two ultrafine particle metrics (UFPN and  $PN_1$ ), and the difference between UFPN and  $PN_1$ . Although motor vehicle emissions are the primary contributors to urban ultrafine particles, these particles are typically emitted initially at sizes around 50 nm and then coagulate to form larger particles (50–120 nm).<sup>31</sup> The UFPN –  $PN_1$  difference tends to reflect particles typically smaller than those from motor vehicle emissions, and has been shown to distinguish ground-level aircraft-related ultrafine particles from those emitted by vehicles.<sup>32,33</sup> Additionally, if “near highway” intersections (those within 1000 m of major highway) are excluded from Figure 4 in this component, a clearer airport signature appears (Figure S2, SI). Therefore, in addition to vehicle emissions, this component is also suggestive of an aircraft-related air pollution source.

The PCA generally showed traffic profiles in Los Angeles comparable to those previously reported in Baltimore.<sup>7</sup> In Baltimore, the first three components indicated sources of diesel exhaust, light-duty vehicle emissions, and crankcase emissions, respectively.<sup>7</sup> Because more than 90% of the annual average daily traffic count in the highway system in the Los Angeles area is due to nontruck vehicles,<sup>34</sup> light-duty vehicle traffic emissions are expected to be one of the primary traffic pollution sources. In particular, gasoline engines have been identified as the primary on-road source of urban VOCs.<sup>35</sup> However, diesel vehicle emissions are also expected to account for a substantial part of the traffic profile. The Health Effects Institute (HEI) has reported that diesel vehicles contributed 32% of the  $PM_{2.5}$  mass in Los Angeles, despite their relatively low numbers compared to gasoline vehicles.<sup>1</sup> Crankcase vent emissions were identified as one of the major traffic-related air pollution sources in both Los Angeles and Baltimore.<sup>7</sup> Crankcase emissions tend to be generated by older heavy-duty diesel vehicles. Both Los Angeles and Baltimore have very busy container ports and have a large amount of heavy-duty truck traffic, with annual truck vehicle miles traveled of 5 283 397 770 miles in the Los Angeles–Long Beach area and 2 345 045 413 miles in Baltimore.<sup>36</sup>

The results here differ from those of Riley et al. in that diesel exhaust does not appear to be the most important source of TRAP in Los Angeles, but it is in Baltimore.<sup>7</sup> California regulates heavy-duty diesel vehicles more strictly: to meet PM and  $NO_x$  emission limits, the California On Road Heavy Duty Diesel Vehicle (In Use) Regulation of 2014 requires most heavy-duty trucks and buses to be equipped with PM filters and newer engines.<sup>37</sup> According to EPA Air Pollutant Emissions Trends Data, the highway traffic emissions have decreased nationwide every year, but the state of California has more rapid decreases than Maryland.<sup>38</sup> For example,  $NO_x$ ,  $PM_{10}$ , and  $PM_{2.5}$  decreased 61%, 34%, and 49% in California during 2007–2016, while they decreased 50%, 12%, and 49% in Maryland, respectively.<sup>32</sup> These larger reductions in TRAP may be attributed to stringent regulations on diesel emissions implemented by the state of California.

An aircraft-related air pollution source was not detected by PCA in Baltimore<sup>7</sup> or by PCA in other previous studies.<sup>39–41</sup> While the Baltimore and Los Angeles airports are approximately equally distant from their respective urban cores, the Los Angeles urban core where most of the monitoring took place is downwind from Los Angeles International Airport (LAX). This, in addition to the different degrees of air traffic at the two airports, may explain why an air traffic component could be identified in Los Angeles but not in Baltimore.

The component score maps (Figure 4) allow one to visualize the spatial distributions of pollution sources. In summer, diesel exhaust and crankcase emissions sources were located downtown and along major roadways, with the spatial distribution being generally similar in the spring. Light-duty vehicle emissions tended to be located downtown and along major roadways in the summer but also spread out in the southern part of the city in the spring. The combustion-related ultrafine particle feature was predominantly high in the southwestern and southern parts of the city near LAX, as well as downtown and along major highways in the summer, but tended to be spread out in the eastern part of the city along highways in the spring. Combustion-related pollutants from heating in the spring could increase the background pollutant concentrations throughout the city and therefore may mask the traffic-related air pollution sources in specific locations in the spring.

A limitation of this study was that the mobile monitoring only took place in the afternoon hours, a period typically characterized by a higher mixing height and therefore better mixing. Not including the morning hours of sampling would have weakened correlations between the mobile and fixed-site monitoring results by not including the time of day when traffic emissions were high and atmospheric mixing depths were relatively low.<sup>42</sup> A comparison of NO<sub>2</sub> concentrations between 2-week average and aggregated afternoon peak hours between 14:00 and 19:00 during the same time period obtained from an AQS monitoring site close to one of our PSD sites supported the perception that NO<sub>2</sub> concentrations during afternoon hours (mean ± SD: 21 ± 12 and 13 ± 5.0 ppb for spring and summer, respectively) were lower than the 2-week average (mean ± SD: 27 ± 13 and 18 ± 10 ppb for spring and summer, respectively). However, NO<sub>2</sub> concentrations during the morning hours between 5:00 and 10:00 (mean ± SD: 30 ± 15 and 23 ± 10 ppb for spring and summer, respectively) were higher than the 2-week average,<sup>24</sup> suggesting that sampling that included both morning and afternoon hours would be more representative of the longer-term average.

It may also have been useful, because of the different traffic characteristics on weekdays than on weekends, to do the PCA on weekday and weekend data separately. Because of limited weekend data, this was not possible in the current study, but might prove useful if sufficient weekend data could be obtained in the future. For example, while weekday traffic congestion is typically the worst in March, weekend congestion is typically the worst in June.<sup>43</sup> Finally, because of the large spatial gradients in the concentrations of some pollutants, it might also be useful to perform similar analyses with shorter buffer lengths for the fuzzy points, such as 100 m, rather than the 300 m as used here. These large spatial gradients may be also responsible for the mobile measurements of NO<sub>2</sub> and NO<sub>x</sub> being consistently lower than the fixed-site measurements in this study, since on average the fixed sites were closer to intersections, which can be traffic pollution “hot spots”, than the mobile measurements.

This study has shown that a campaign of combined mobile and fixed-site monitoring can be used to identify source profiles of traffic-related and aircraft-related emissions, as well as the intraurban spatial distributions of those source emissions. Combined with the results of Riley et al.,<sup>7</sup> we have shown this approach to be applicable in multiple cities. This study uses the approach of applying APCS to investigate spatial patterns in emission sources. In the future, this approach and the resulting spatial information could be used with other spatial data, such as the locations of roads or other land uses, for source-specific pollution exposure estimation.

## Supplementary Material

Refer to Web version on PubMed Central for supplementary material.

## Acknowledgments

This publication was made possible by a USEPA grant (RD-83479601-0). Its contents are solely the responsibility of the grantee and do not necessarily represent the official views of the USEPA. Further, the USEPA does not endorse the purchase of any commercial products or services mentioned in the publication. Additional support was provided by the National Institute of Environmental Health Sciences sponsored University of Washington Biostatistics, Epidemiologic and Bioinformatic Training in Environmental Health (BEBTEH) Training Grant (T32ES015459). This publication's contents are solely the responsibility of the authors and do not necessarily represent the official views of the sponsoring agencies.

## References

1. Traffic-Related Air Pollution: A Critical Review of the Literature on Emissions, Exposure, and Health Effects; Special Report 17. Health Effects Institute; Boston, MA: 2010. <https://www.healtheffects.org/publication/traffic-related-air-pollution-critical-review-literature-emissions-exposure-and-health>
2. Fitz, DR., Bumiller, K., Etyemezian, V., Kuhns, H., Nikolich, G. Measurement of PM<sub>10</sub> emission rate from roadways in Las Vegas, Nevada using a SCAMPER mobile platform with real-time sensors. 14th International Emission Inventory Conference, Las Vegas, Nevada, April 12–14, 2005. 2005. <http://citeseerx.ist.psu.edu/viewdoc/download?doi=10.1.1.565.4196&rep=rep1&type=pdf>
3. Marc M, Zabiegala B, Namiesnik J. Mobile systems (portable, handheld, transportable) for monitoring air pollution. *Crit. Rev. Anal. Chem.* 2012; 42(1):2–15.
4. Dons E, Temmerman P, Van Poppel M, Bellemans T, Wets G, Panis LI. Street characteristics and traffic factors determining road users' exposure to black carbon. *Sci. Total Environ.* 2013; 447:72–79. [PubMed: 23376518]
5. Van den Bossche J, Peters J, Verwaeren J, Botteldooren D, Theunis J, De Baets B. Mobile monitoring for mapping spatial variation in urban air quality: development and validation of a methodology based on an extensive dataset. *Atmos. Environ.* 2015; 105:148–161.
6. Adar SD, Gold DR, Coull BA, Schwartz J, Stone PH, Suh H. Focused exposures to airborne traffic particles and heart rate variability in the elderly. *Epidemiology.* 2007; 18:95–103. [PubMed: 17149139]
7. Riley E, Schaal L, Sasakura M, Crampton R, Gould T, Hartin K, Sheppard L, Larson T, Simpson C, Yost M. Correlations between short-term mobile monitoring and long-term passive sampler measurements of traffic-related air pollution. *Atmos. Environ.* 2016; 132:229–239.
8. Sekine K, Shima M, Nitta Y, Adachi M. Long term effects of exposure to automobile exhaust on the pulmonary function of female adults in Tokyo, Japan. *Occup. Environ. Med.* 2004; 61:350–357. [PubMed: 15031394]
9. Westerdahl D, Fruin S, Sax T, Fine PM, Sioutas C. Mobile platform measurements of ultrafine particles and associated pollutant concentrations on freeways and residential streets in Los Angeles. *Atmos. Environ.* 2005; 39(20):3597–3610.

10. Brantley HL, Hagler GSW, Kimbrough ES, Williams RW, Mukerjee S, Neas LM. Mobile air monitoring data-processing strategies and effects on spatial air pollution trends. *Atmos. Meas. Tech.* 2014; 7:2169–2183.
11. Rivera M, Basagaña X, Aguilera I, Agis D, Bouso L, Foraster M, Medina-Ramón M, Pey J, Künzli N, Hoek G. Spatial distribution of ultrafine particles in urban settings: A land use regression model. *Atmos. Environ.* 2012; 54:657–666.
12. Hankey S, Marshall JD. Land Use Regression Models of On-Road Particulate Air Pollution (Particle Number, Black Carbon, PM<sub>2.5</sub>, Particle Size) Using Mobile Monitoring. *Environ. Sci. Technol.* 2015; 49:9194–9202. [PubMed: 26134458]
13. Montagne DR, Hoek G, Klompaker JO, Wang M, Meliefste K, Brunekreef B. Land Use Regression Models for Ultrafine Particles and Black Carbon Based on Short-Term Monitoring Predict Past Spatial Variation. *Environ. Sci. Technol.* 2015; 49:8712–8720. [PubMed: 26079151]
14. Apte JS, Messier KP, Gani S, Brauer M, Kirchstetter TW, Lunden MM, Marshall JD, Portier CJ, Vermeulen RCH, Hamburg SP, Hamburg SP. High-Resolution Air Pollution Mapping with Google Street View Cars: Exploiting Big Data. *Environ. Sci. Technol.* 2017; 51:6999–7008. [PubMed: 28578585]
15. Kerckhoffs J, Hoek G, Messier KP, Brunekreef B, Meliefste K, Klompaker JO, Vermeulen R. Comparison of Ultrafine Particle and Black Carbon Concentration Predictions from a Mobile and Short-Term Stationary Land-Use Regression Model. *Environ. Sci. Technol.* 2016; 50:12894–12902. [PubMed: 27809494]
16. Kerckhoffs J, Hoek G, Vlaanderen J, van Nunen E, Messier K, Brunekreef B, Gulliver J, Vermeulen R. Robustness of intra urban land-use regression models for ultrafine particles and black carbon based on mobile monitoring. *Environ. Res.* 2017; 159:500–508. [PubMed: 28866382]
17. Sullivan R, Pryor S. Quantifying spatiotemporal variability of fine particles in an urban environment using combined fixed and mobile measurements. *Atmos. Environ.* 2014; 89:664–671.
18. Larson T, Henderson SB, Brauer M. Mobile monitoring of particle light absorption coefficient in an urban area as a basis for land use regression. *Environ. Sci. Technol.* 2009; 43:4672–4678. [PubMed: 19673250]
19. Riley EA, Banks L, Fintzi J, Gould TR, Hartin K, Schaal L, Davey M, Sheppard L, Larson T, Yost MG, Simpson CD. Multi-pollutant mobile platform measurements of air pollutants adjacent to a major roadway. *Atmos. Environ.* 2014; 98:492–499.
20. Larson T, Gould T, Riley EA, Austin E, Fintzi J, Sheppard L, Yost M, Simpson C. Ambient air quality measurements from a continuously moving mobile platform: Estimation of area-wide, fuel-based, mobile source emission factors using absolute principal component scores. *Atmos. Environ.* 2017; 152:201–211.
21. Kolb CE, Herndon SC, McManus B, Shorter JH, Zahniser MS, Nelson DD, Jayne JT, Canagaratna MR, Worsnop DR. Mobile laboratory with rapid response instruments for real-time measurements of urban and regional trace gas and particulate distributions and emission source characteristics. *Environ. Sci. Technol.* 2004; 38:5694–5703. [PubMed: 15575289]
22. Comrey, AL., Lee, HB. *A First Course in Factor Analysis*. 2. Lawrence Erlbaum Associates; Hillsdale, NJ: 1992.
23. R Development Core Team. *R: A Language and Environment for Statistical Computing*. R Foundation for Statistical Computing; Vienna, Austria: 2008. <http://www.R-project.org>
24. U.S. Environmental Protection Agency. Air Quality System (AQS) Data Mart. 2013. [https://aq5.epa.gov/aqsweb/documents/data\\_mart\\_welcome.html](https://aq5.epa.gov/aqsweb/documents/data_mart_welcome.html)
25. Borbon A, Gilman J, Kuster W, Grand N, Chevaillier S, Colomb A, Dolgorouky C, Gros V, Lopez M, SardaEsteve R, Holloway JS, Stutz J, Petetin H, McKeen S, Beekmann M, Warneke C, Parrish D, De Gouw J. Emission ratios of anthropogenic volatile organic compounds in northern mid-latitude megacities: observations versus emission inventories in Los Angeles and Paris. *J. Geophys. Res.-Atmos.* 2013; 118:2041–2057.
26. Oakes MM, Baxter LK, Duvall RM, Madden M, Xie MJ, Hannigan MP, Peel JL, Pachon JE, Balachandran S, Russell A, Long TC. Comparing multipollutant emissions-based mobile source

- indicators to other single pollutant and multipollutant indicators in different urban areas. *Int. J. Environ. Res. Public Health*. 2014; 11(11):11727–11752. [PubMed: 25405595]
27. Fruin S, Westerdaal D, Sax T, Sioutas C, Fine PM, Fine PM. Measurements and predictors of onroad ultrafine particle concentrations and associated pollutants in Los Angeles. *Atmos. Environ.* 2008; 42:207–219.
  28. Dallmann T, Kirchstetter T, DeMartini S, Harley R. Quantifying on-road emissions from gasoline-powered motor vehicles: accounting for the presence of medium- and heavy-duty diesel trucks. *Environ. Sci. Technol.* 2013; 47:13873–13881. [PubMed: 24215572]
  29. Zielinska B, Campbell D, Lawson DR, Ireson RG, Weaver CS, Hesterberg TW, Larson T, Davey M, Liu LJS. Detailed characterization and profiles of crankcase and diesel particulate matter exhaust emissions using speciated organics. *Environ. Sci. Technol.* 2008; 42(15):5661–5666. [PubMed: 18754490]
  30. Shirmohammadi F, Wang DB, Hasheminassab S, Verma V, Schauer JJ, Shafer MM, Sioutas C. Oxidative potential of onroad fine particulate matter (PM<sub>2.5</sub>) measured on major freeways of Los Angeles, CA, and a 10-year comparison with earlier roadside studies. *Atmos. Environ.* 2017; 148:102–114.
  31. Xiong C, Friedlander SK. Morphological properties of atmospheric aerosol aggregates. *Proc. Natl. Acad. Sci. U. S. A.* 2001; 98:11851–11856. [PubMed: 11592995]
  32. Riley EA, Gould T, Hartin K, Fruin SA, Simpson CD, Yost MG, Larson T. Ultrafine particle size as a tracer for aircraft turbine emissions. *Atmos. Environ.* 2016; 139:20–29.
  33. Shirmohammadi F, Sowlat MH, Hasheminassab S, Saffari A, Ban-Weiss G, Sioutas C. Emission rates of particle number, mass and black carbon by the Los Angeles International Airport (LAX) and its impact on air quality in Los Angeles. *Atmos. Environ.* 2017; 151:82–93.
  34. 2013 Annual Average Daily Truck Traffic on the California State Highway System. California Department of Transportation; Sacramento, CA: 2016. [http://www.dot.ca.gov/trafficops/census/docs/2013\\_aadt\\_truck.pdf](http://www.dot.ca.gov/trafficops/census/docs/2013_aadt_truck.pdf)
  35. Gentner DR, Jathar SH, Gordon TD, Bahreini R, Day DA, El Haddad I, Hayes PL, Pieber SM, Platt SM, de Gouw J, Goldstein AH, Harley RA, Jimenez JL, Prévôt ASH, Robinson AL. Review of urban secondary organic aerosol formation from gasoline and diesel motor vehicle emissions. *Environ. Sci. Technol.* 2017; 51:1074–1093. [PubMed: 28000440]
  36. Bronzini, M. Relationships Between Land Use and Freight and Commercial Truck Traffic in Metropolitan Areas; Special Report 298. Transportation Research Board: Washington, DC; 2008. <http://onlinepubs.trb.org/onlinepubs/sr/sr298bronzini.pdf>
  37. Truck and Bus Regulation 2014: Appendix B. Existing Regulation Summary. California Air Resources Board (ARB), California Environmental Protection Agency; Sacramento, CA: 2016.
  38. State Average Annual Emissions Trend 1990–2016. U.S. Environmental Protection Agency; Washington, DC: 2017. <https://www.epa.gov/air-emissions-inventories/air-pollutant-emissions-trends-data>.
  39. Bruno P, Caselli M, de Gennaro G, Traini A. Source apportionment of gaseous atmospheric pollutants by means of an absolute principal component scores (APCS) receptor model. *Fresenius' J. Anal. Chem.* 2001; 371:1119–1123. [PubMed: 11798109]
  40. Viana M, Querol X, Alastuey A, Gil JI, Menéndez M. Identification of PM sources by principal component analysis (PCA) coupled with wind direction data. *Chemosphere*. 2006; 65:2411–2418. [PubMed: 16766018]
  41. Chan TW, Mozurkewich M. Application of absolute principal component analysis to size distribution data: identification of particle origins. *Atmos. Chem. Phys.* 2007; 7:887–897.
  42. Frey, HC., Grieshop, A., Roupail, N., Fuentes, M., Khlystov, A., Bangs, J., Rodriquez, D. Characterizing the determinants of vehicle traffic emissions exposure: Measurements and modeling of land-use, traffic, emissions, transformation and transport. Health Effects Institute 2017 Annual Conference, Alexandria, Virginia, Apr 30–May 2. 2017. <https://www.healtheffects.org/research/ongoing-research/characterizing-determinants-vehicle-traffic-emissions-exposure>

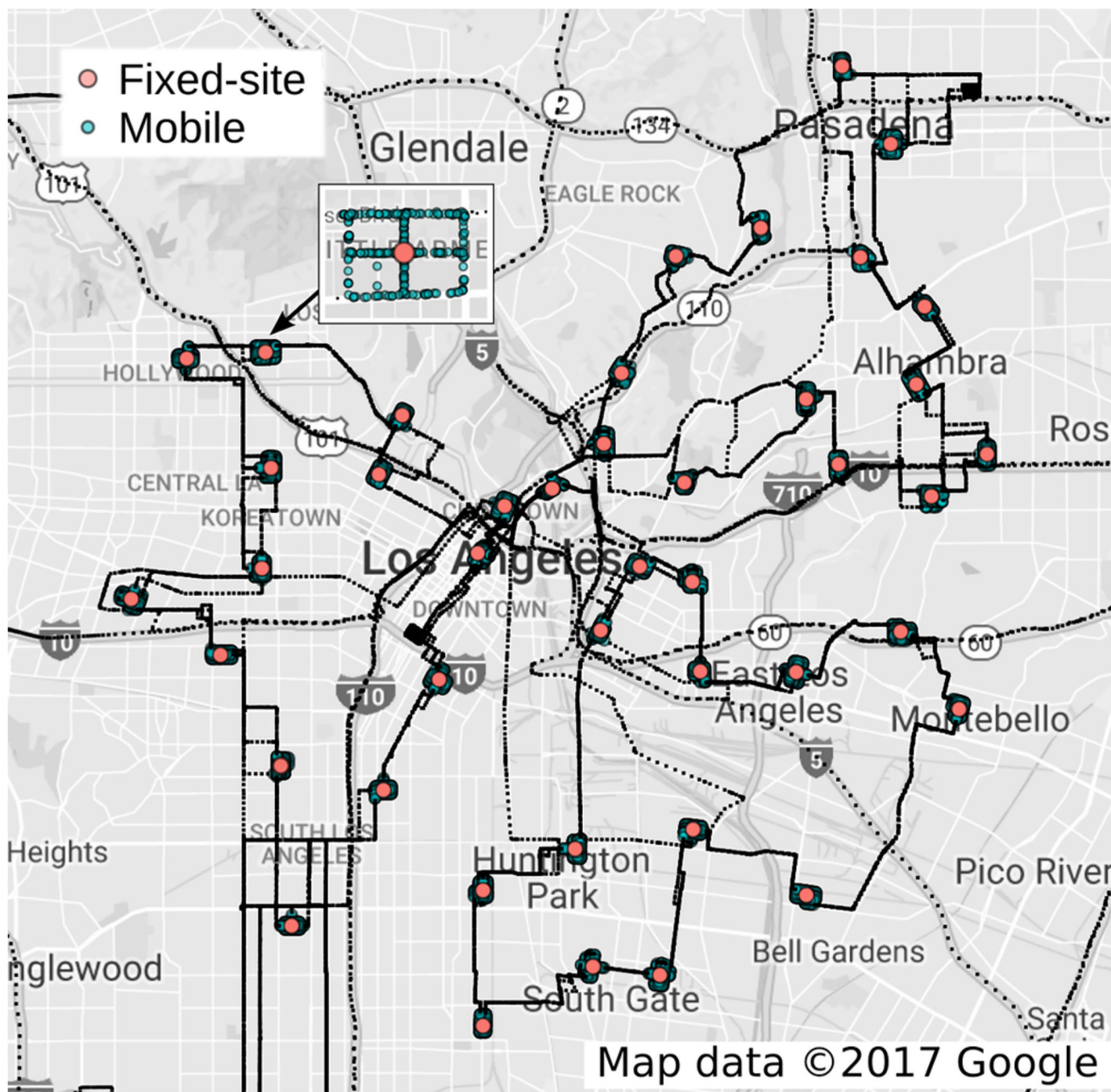
43. Memmott, J., Young, P. *Seasonal Variation in Traffic Congestion: A Study of Three U.S. Cities*, Bureau of Transportation Statistics Technical Reports August 2008. United States Department of Transportation; Washington, DC: 2008. <http://www.trb.org/Main/Blurbs/160230.aspx>

Author Manuscript

Author Manuscript

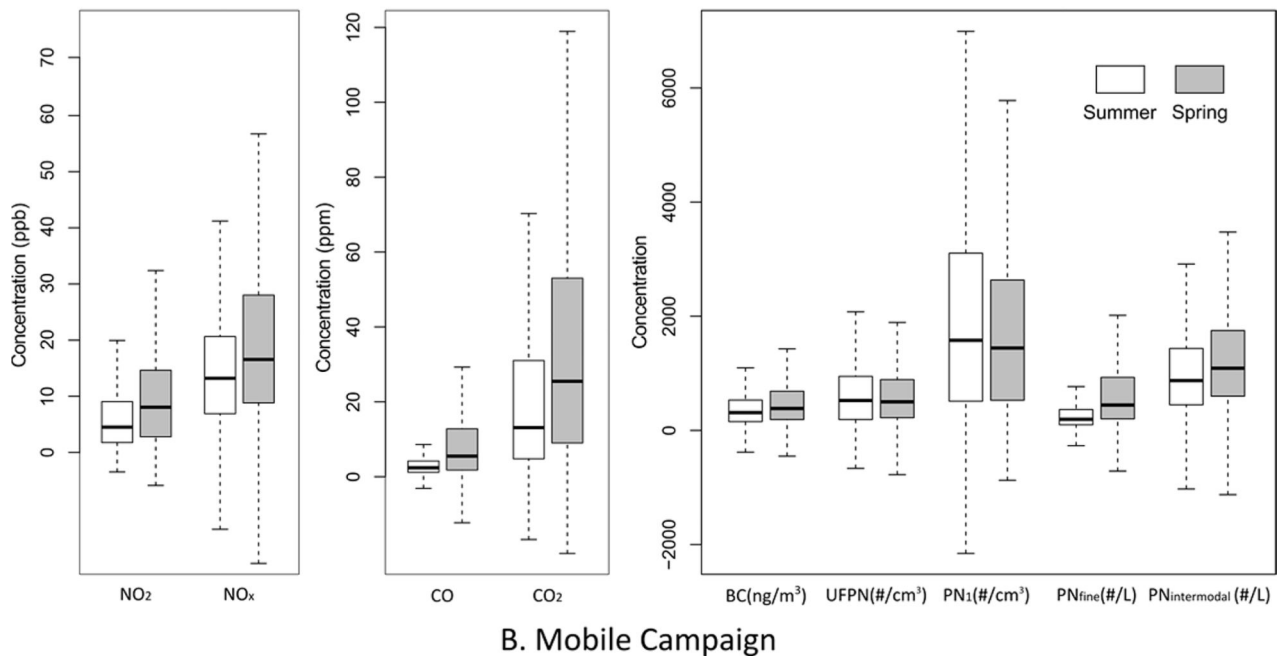
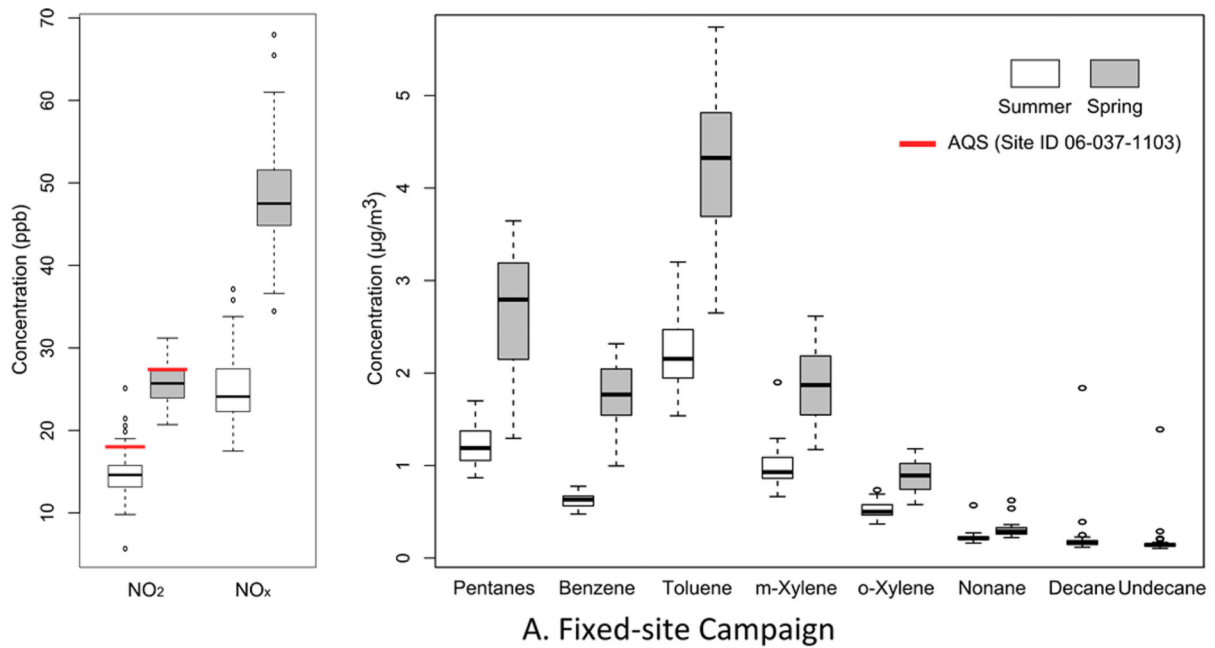
Author Manuscript

Author Manuscript



**Figure 1.**

Locations of 43 fuzzy points with the fixed sites (in red) and mobile sampling sites within a 300 m radius around each intersection (in blue) in the summer campaign. Black lines connecting the fuzzy points indicate the continuous mobile route. The inset near the top left shows an enlarged map of one of the fuzzy points.

**Figure 2.**

Distribution of pollutant concentrations. Fixed-site platform results are shown at the top (A) and mobile platform results are shown at the bottom (B). Pentanes are divided by 100 and include pentanes and hexanes. Dodecane and undecane are not available in spring due to measurements below the limit of detection (LOD) and/or the limit of quantification (LOQ). CO measurements are multiplied by 10, UFPN measurements are divided by 10, and  $PN_{\text{fine}}$  measurements are divided by 100. The AQS measurements of  $NO_2$  for the same period of time in central Los Angeles (GPS 34.066590,  $-118.226880$ ) are shown as red lines in part A. Some outliers are not displayed in the figure to facilitate visual comparison.



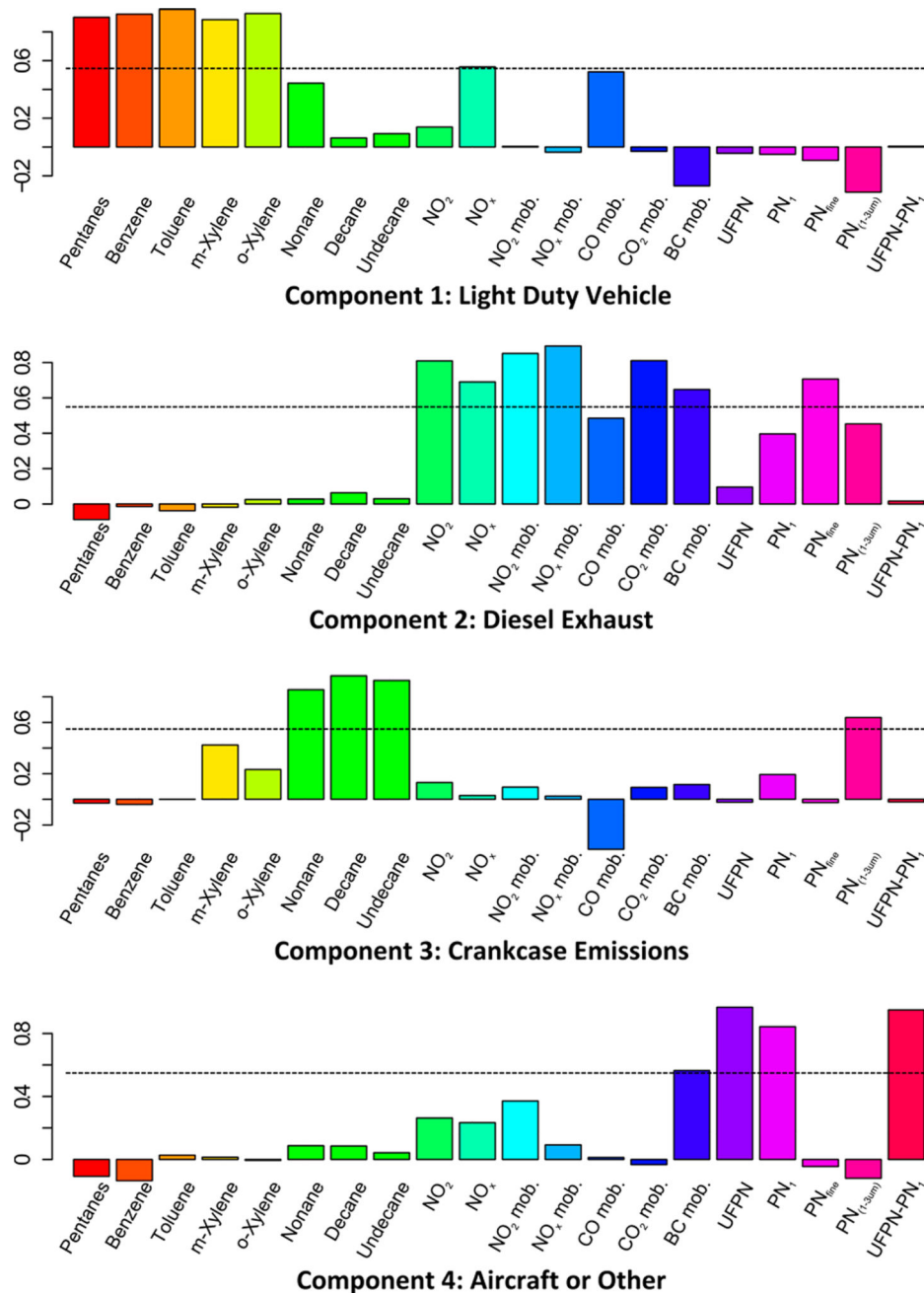


**Figure 3.** Principal components analyses with varimax rotation for the combined mobile and fixed-site data. Loadings of four rotated components with assigned sources are shown in the bar charts. High loading refers to loadings that are greater than 0.55 (i.e., those bars above the black dash line).

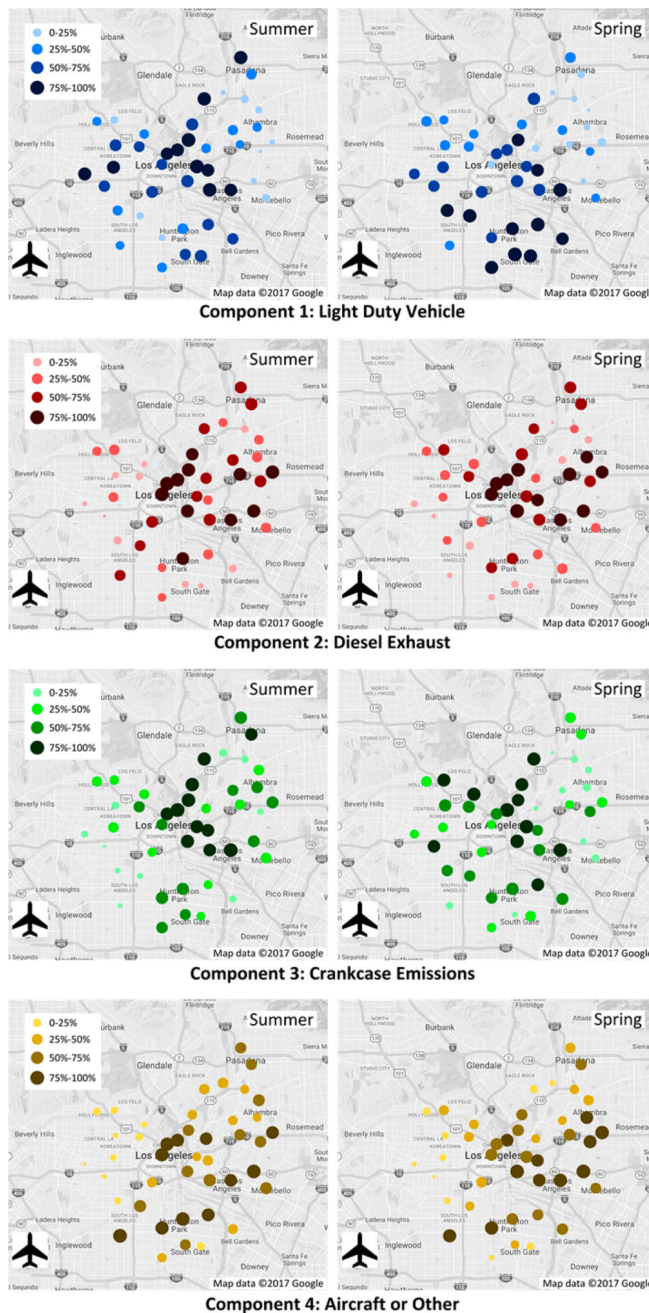


**Figure 4.** Percentiles of scores for each absolute PCA component with its assigned source at each location are shown in the maps for the summer (left) and spring (right) campaigns. On these maps, larger and darker circles indicate larger contributions to pollutant concentrations.

**Table 1**

Summary of Prominent Components of PCA for the Combined Mobile and Fixed-Site Data

component	explained variance (%)	high loading pollutants	likely source
1st	26	low molecular weight hydrocarbons, xylenes, NO <sub>x</sub>	light-duty vehicle
2nd	24	NO <sub>2</sub> , NO <sub>x</sub> , CO <sub>2</sub> , BC, PN <sub>fine</sub>	diesel exhaust
3rd	17	long-chain alkanes, PN <sub>intermodal</sub>	crankcase emissions
4th	16	UFPN, PN <sub>1</sub> , UFPN – PN <sub>1</sub> , BC	aircraft or other

Author Manuscript

Author Manuscript

Author Manuscript

Author Manuscript